HHS Public Access

Author manuscript

J Mol Cell Cardiol. Author manuscript; available in PMC 2015 December 01.

Published in final edited form as:

J Mol Cell Cardiol. 2014 December ; 77: 86–101. doi:10.1016/j.yjmcc.2014.09.011.

MMI-0100 inhibits cardiac fibrosis in myocardial infarction by direct actions on cardiomyocytes and fibroblasts via MK2 inhibition

Lei Xu, MD, MS[1], **Cecelia C. Yates, PhD**[2], **Pamela Lockyer, BS**[3], **Liang Xie, PhD**[4], **Ariana Bevilacqua, BS**[3], **Jun He, MD, PhD**[3,5], **Cynthia Lander, PhD**[6], **Cam Patterson, MD, MBA**[6,7,8], and **Monte Willis, MD, PhD**[3,8,*]

[1]Department of Cardiac Surgery, Shandong Provincial Hospital affiliated to Shandong University

[2]Department of Health Promotions and Development, School of Nursing, University of Pittsburgh, Pittsburgh, PA USA

[3]Department of Pathology & Laboratory Medicine, University of North Carolina, Chapel Hill, NC USA

[4]Department of Medicine, University of North Carolina, Chapel Hill, NC USA

[5]General Hospital of Ningxia Medical University, Yichuan, Ningxia, P. R. China

[6]Moerae Matrix, 55 Madison Avenue Suite 400, Morristown, NJ 07960

[7]Departments of Cell and Developmental Biology, Medicine, and Pharmacology, University of North Carolina, Chapel Hill, NC USA

[8]McAllister Heart Institute, University of North Carolina, Chapel Hill, NC USA

Abstract

The cell-permeant peptide inhibitor of MAPKAP kinase 2 (MK2), MMI-0100, inhibits MK2 and downstream fibrosis and inflammation. Recent studies have demonstrated that MMI-0100 reduces intimal hyperplasia in a mouse vein graft model, pulmonary fibrosis in a murine bleomycin-induced model and development of adhesions in conjunction with abdominal surgery. MK2 is critical to the pathogenesis of ischemic heart injury as MK2 −/− mice are resistant to ischemic remodeling. Therefore, we tested the hypothesis that inhibiting MK2 with MMI-0100 would protect the heart after acute myocardial infarction (AMI) in vivo. AMI was induced by placing a permanent LAD coronary ligation. When MMI-0100 peptide was given 30 minutes after permanent LAD coronary artery ligation, the resulting fibrosis was reduced/prevented ~50% at a 2

*Corresponding author: Monte S. Willis, MD, PhD, Associate Professor, McAllister Heart Institute, Department of Pathology & Laboratory Medicine, University of North Carolina, 111 Mason Farm Road, MBRB 2340B, Chapel Hill, NC 27599, Phone: (919) 843-1938, FAX: (919) 843-4585, monte_willis@med.unc.edu.

Disclosures

Cynthia Lander is Chairman and CEO of Moerae Matrix, Inc. L.Xu, P.L., L.Xie, A.B., J.H., C.P., and M.W. report no conflict of interest.

week time point, with a corresponding improvement in cardiac function and decrease in left ventricular dilation. In cultured cardiomyocytes and fibroblasts, MMI-0100 inhibited MK2 to reduce cardiomyocyte caspase 3/7 activity, while enhancing primary cardiac fibroblast caspase 3/7 activity, which may explain MMI-0100's salvage of cardiac function and anti-fibrotic effects in vivo. These findings suggest that therapeutic inhibition of MK2 after acute MI, using rationally-designed cell-permeant peptides, inhibits cardiac fibrosis and maintains cardiac function by mechanisms that involve inhibiting cardiomyocyte apoptosis, while enhancing primary cardiac fibroblast cell death.

Keywords

apoptosis; cardiac ischemia; cardiomyocytes; fibroblast; fibrosis; MAPKAP kinase 2; MK2; MMI-0100; necrosis

Introduction

Ischemic heart disease is the most common cause of death in the world; in the United States alone, an estimated 785,000 people will have a myocardial infarction (MI) each year, approximately 1 per minute [1]. The adverse remodeling that occurs after MI contributes to the impaired function and heart failure that commonly develops post-MI. Interventional advances - largely early reperfusion therapies - have improved patient survival, but the adverse remodeling processes that lead to heart failure proceed unabated [2–4]. The size of the infarcted area, the infarcted wound healing, and chronic left ventricular (LV) remodeling determine the extent of the resulting heart failure [2–4]. To minimize the extent of heart failure after a large or recurrent MI, therapeutic strategies are needed to limit infarct wound healing in the early phase.

Use of rationally designed cell-permeant peptides that inhibit Mitogen Activated Protein Kinase Activated Protein Kinase II (MK2) activity and downstream fibrosis and inflammation is a unique approach. Recent studies have reported that the cell-permeant peptide MMI-0100 inhibits inflammation and fibrosis (intimal hyperplasia) in a mouse vein graft model [5], bleomycin-induced pulmonary fibrosis [6] and abdominal adhesions post-surgery [7]. These peptide drugs target the substrate-binding site of MK2, are carried into cells via cell-permeant domains and are rapidly taken up by macropinocytosis and targeted to endosomal compartments, where they are retained for up to 7 days [8]. MK2 is critical for both fibrosis and inflammation; therefore, MK2-driven processes central to the exuberant cardiac fibrosis and cytokine release that occur post-myocardial infarction remodeling represent an excellent therapeutic target.

Myocyte death during lethal myocardial infarction, cardiac dysfunction, and fibrosis during post-MI remodeling and hypertrophy are associated with sustained activation of p38 [9–11]. Recent studies in MK2 −/− mice have illustrated that MK2 acts downstream of p38 and is responsible for p38-induced heart failure [12]. Similarly, MK2 −/− mice are resistant to ischemia reperfusion injury [13], indicating a critical role of MK2 in ischemic heart disease experimentally. Based on these recent findings, the present study tested the hypothesis that MMI-0100 therapy *post*-myocardial infarction would inhibit the extent of fibrosis *in vivo*.

We demonstrated that MMI-0100 reduced fibrosis that developed after 2 weeks in a standard murine myocardial infarction model induced by permanent ligation of the left anterior descending (LAD) coronary artery. Since cardiomyocyte cell death, fibroblast differentiation to myofibroblasts and the secretion of a variety of extracellular matrix proteins, including collagen (resulting in fibrosis) are impacted by MK2, we determined whether MMI-0100 confers cardioprotective benefits by acting on both cell types independently in vitro. We found that MMI-0100 inhibits MK2 activity in both cardiac-derived cells (H9C2 and HL-1) and in primary rat cardiac fibroblasts, inhibiting cardiomyocyte caspase 3/7 activity, while enhancing fibroblast caspase 3/7 activity in vitro. These studies report for the first time that the cell-permeant peptide MMI-0100 can inhibit fibrosis associated with myocardial infarction, while illustrating mechanisms by which inhibition of MK2 in turn inhibits cardiomyocyte apoptosis and reduces fibrosis by direct effects on cardiac fibroblasts.

Materials and Methods

Cell permeant peptide synthesis and delivery

The MMI-0100 peptide (YARAAARQARAKALARQLGVAA) was synthesized using standard Fmoc chemistry, as previously described [14]. MMI-0100 (MW=2283.67g/mol; Moerae Matrix, Inc.) was prepared and delivered daily intraperitoneally in PBS (50 μg/kg), as previously described [6]. In cell line studies, the peptide was dissolved in DMSO before adding to the cell media (final [0.5%] to target peptide intracellularly), as previously described [7], to give a final MMI-0100 concentration of 20 μM or 100 μM.

Animals and myocardial infarction (MI) model

Twelve week-old male C57BL/6 mice (25–30 g) were obtained from Jackson Laboratories (Bar Harbor, ME) and maintained in the University of North Carolina at Chapel Hill facilities for at least 7 days with free access to standard rodent food and water. Myocardial infarction was induced by permanent ligation of the left anterior descending (LAD) coronary artery as described previously [15, 16]. Post-surgery, mice were immediately treated with lidocaine (6 mg/kg IM) and atropine (0.04–0.10 mg/kg IM) upon surgical closure, followed by lidocaine and atropine every 2–4 hours for the first 24 hours to prevent arrhythmias. Post-anesthesia, mice were given 0.1mg/kg buprenorphine every 12 hours for the first 48 hours. Within the first hour post-MI, 50 μg/kg/day MMI-0100 peptide (or PBS control) was given intraperitoneally and repeated for a total of 14 days. In parallel, control groups underwent: 1) a sham operation that included every step except the coronary artery ligation; 2) daily MMI-0100 (50 μg/kg/day) intraperitoneally for 14 days. Cardiac function was measured by conscious echocardiography using a Vevo 2100 ultrasound biomicrscopy system (VisualSonics, Inc., Toronto, Canada) at baseline, 7, and 14 days, as previously described [17–19].

Histological analysis of fibrosis

Mice were euthanized by isoflurane and cervical dislocation at day 14, fixed in fresh 4% paraformaldehyde for 24 hours, paraffin-embedded, processed, and stained with standard hematoxylin and eosin (H&E) and Masson's trichrome (MT). Starting at the ligation with fully faced tissue, 14–15 levels were cut on each block at 50 μm (one slide for H&E, one for

MT, and 3 unstained; 50 μm skipped and then repeated). Controls were similarly cut starting at a comparable level. The area of fibrosis was analyzed in 3–4 blindly chosen hearts, each heart at 14–15 levels (point of ligation to apex), 3 sections at each level. Analysis of collagen was performed blinded to treatment on these 42–45 sections per heart. Slides were scanned using an Aperio ScanScope (Aperio Technologies, Vista, CA) and analyzed using Aperio ImageScope. The Algorithm Positive Pixel Count v9 was used to measure the Masson's trichrome staining of collagen (representing both fibrosis and collagen in extracellular matrix), hue value (0.66) and hue width (0.1) were used analyzed the tissue outlined using the pen tool. Each section was analyzed and exported. The N positive/N total value (representing the % collagen of the entire section) was used to determine a weighted average for each slide.

Immunofluorescence staining of cardiac histological sections for vimentin, αSMA, TGF-β1 and TUNEL

Immunostaining was performed as described previously [20, 21]. Cardiac sections adjacent to histological levels 1 and 7 (of 14-see histological analysis of fibrosis) were stained with antibodies against α-SMA (1:250, Abcam, Cambridge, MA), Vimentin (1:100, Santa Cruz, Dallas, TX), and TGF-β-1 (1:100, Abcam), or an irrelevant isotype mouse, rabbit or goat IgG (as a negative control) at 4°C overnight. Slides were then incubated with Alexa Fluor 488-conjugated secondary antibodies and counterstained with 4,6-diamidino-2-phenylindole (DAPI) (Vector Laboratories, Burlingame, CA).

Identification of apoptosis was determined in histological sections by identifying the presence of fragmented DNA by terminal deoxynucleotidyl transferase dUTP nick end labeling (TUNEL) using the Roche TUNEL in situ staining kit (Roche Molecular Biochemicals, Basel, Switzerland), according to the manufacturer's instructions. To detect DNA fragmentation associated with apoptosis, we used a fluorescence-based TUNEL followed by counterstaining with 4,6-diamidino-2-phenylindole (DAPI). Histological sections treated with a recombinant DNase I to allow TUNEL labeling of all nuclei were used as positive controls.

Cell culture of primary cardiac fibroblast cells and cardiomyocyte cell lines

The H9C2 is a myoblast cell line derived from rat myocardium obtained from ATCC® (CRL-1446, ATCC, Manassas, VA) and cultured according to the recommended protocols. Briefly, cells (p2) were maintained at 37°C with 5% CO2 in DMEM supplemented with 10% fetal bovine serum and antibiotics (100 U/ml penicillin, 100 mg/ml streptomycin) and split at a ratio of 1:4 using 0.05% trypsin every 36 hours. HL-1 cells were obtained from Dr. William Claycomb and cultured according to the published protocols [22, 23]. Briefly, cells (p67) were cultured in Claycomb medium (JRH Biosciences, USA) supplemented with 10% fetal bovine serum (JRH Biosciences), 2 mM L-glutamine (Gibco, Grand Island, NY), 100 μM norepinephrine (Sigma, USA), 100 U/mL penicillin, and 100 μg/mL streptomycin (Gibco) in flasks precoated with fibronectin and gelatin (Sigma), then incubated at 37°C in 5% CO_2. Cells were split at a ratio of 1:4 using 0.05% trypsin every 48 hours. Primary cardiac fibroblasts were obtained from 2–4-day-old Sprague Dawley® rats, according to previously described protocols (primary cardiomyocyte isolation kit, cat.#LK003300,

Worthington Biochemical Corp., Lakewood, NJ) [24, 25]. Harvested fibroblasts (p2) were seeded in 10 cm FALCON polystyrene dishes (BD Biosciences), and incubated for 45 min in DMEM with 10% fetal bovine serum and antibiotics. Cardiomyocytes that did not attach to the non-coated plates were rinsed away and the remaining fibroblasts were given fresh medium, grown to confluence, trypsinized (0.05%) and passaged twice before being used in experiments.

Induction of hypoxia and determination of cell death in vitro and effects of MMI-0100 given at the start of ischemia time

Cells were rinsed in PBS and grown in DMEM (cat.#11966-025, Gibco) for 2 hours prior to initiating hypoxia (simulated ischemia). Hypoxia was induced by placing cells in a hypoxia chamber (HERACELL 150i, Thermo Scientific) in a mixture of 5% CO_2/95% N_2 to attain a 1% oxygen concentration, according to the manufacturer's instruction. Three experimental groups were tested for each cell type: 1) Final [0.5% DMSO]; 2) 20 μM MMI-0100 peptide [in a final 0.5% DMSO]; and 3) 100μM MMI-0100 peptide [in a final 0.5% DMSO] at 3 time points. The MMI-0100 peptide was added to the cells at the start of the ischemia time. Cells were cultured in 12 well plates. At the time of performing the experiments, all cultures were approximately 70–90% confluent. 3 different time points were adopted for each of the 3 cell lines according to the severity of cell death under hypoxia determined by LDH release: for H9C2 cell line: 8hr; 16hr; 24hr; for HL-1 cell line: 4hr; 8hr; 12hr; for cardiac fibroblast cell line: 16hr; 32hr; 48hr.

Cell death was first determined using an LDH release assay (cat.#630117, Clontech), according to the manufacturer's instructions. Briefly, after MMI-0100 peptide treatment and challenge with hypoxia (or normoxia control) conditions, 100 μl of culture medium was assayed for LDH release using LDH assay kits; in parallel, 100 μl of the Catalyst and the Dye were assayed and read at 490 nm (CLARIOstar, BMG LABTECH GmbH, Ortenberg, Germany). All data were run in triplicate and presented as a percentage of parallel cells treated with a final of 1%Triton-X-100. Caspase 3/7 activity was next determined using a commercial Caspase 3/7 activity kit (cat.#G8091, Promega, Madison, WI 53711) in a 384 well plate (cat.#781903, Greiner bio-one) according to the manufacturer's instructions. Briefly, cells were harvested in 35 μl ice cold Passive Lysis Buffer (cat.#E194A, Promega), rocked for 5 min at RT, then stored at −80C. The resulting cell lysates were centrifuged at 10,000 ×g for 10 min. The resulting cell lysates (25 μl, with 0.6ug total protein) and Caspase-Glo 3/7 Reagent were added to each well in a 1:1 ratio and the luminescence was read (CLARIOstar, BMG LABTECH GmbH).

Immunoblot analysis of MK2 activity

Leftover cell lysates from the Caspase activity assay were used for Western blots. Cell lysate was first fractionated by SDS-4~10% polyacrylamide gel electrophoresis and transferred to PVDF membranes (cat.#162-0177, Bio-Rad, Berkeley, California). After blocking with recommended blocking reagents for 1h at room temperature, membranes were incubated overnight at 4°C with primary antibodies in TBS-T, then incubated with secondary antibodies conjugated with HRP in TBS-T. hnRNPA0, MAPK2, and phospho-MAPK2 proteins were detected using anti-hnRNPA0 (cat.#HPA036569, 1:1000, Sigma-Aldrich),

anti-MAPKAPK2 (cat.#SAB4300553, Sigma-Aldrich) and anti-phospho-MAPKAPK2 (cat.#SAB4300241, 1:1000, Sigma-Aldrich). As a loading control, βactin was detected using anti-βactin (cat.#A2228, 1:6000, Sigma-Aldrich). Goat anti-rabbit IgG (whole molecule)–Peroxidase antibody (cat.#A9169, 1:1000, Sigma-Aldrich) and anti-Mouse IgG (Fab specific)–Peroxidase antibody produced in goat (cat.#A9917, 1:6000, Sigma-Aldrich) were used as secondary antibodies. Lumigen ECL Ultra (cat.#TMA-100, Lumigen, Southfield, MI) chemiluminescence was detected using the BioSpectrum Imaging System (Biospectrum 510, UVP, Upland, CA). Quantity One 1-D Analysis Software (cat.#170-9600, Bio-Rad Laboratories, Inc., Hercules, CA) was utilized for densitometry analysis.

Cytokine analysis of cell media for TNFα, IL-1β, and IL-6

Cytokine analysis of TNFα, IL-1β, and IL-6 was performed for either mouse (HL1) or rat (H9C2 and primary cardiac fibroblasts) using Luminex multiplex assays (LUM000, LUM401, LUM406, LUM410, LUR000, LUR401, LUR406, LUR410, R&D Systems, Inc., Minneapolis, MN) run on a Bio-Plex 200 (Bio-Rad, Hercules, CA) using standard curves run in parallel with each experiment.

Statistical analysis

SigmaPlot (Systat Software, Inc., San Jose, CA) was used to determine statistical significance for survival, physiology, in vitro studies, and histology. Differences in survival curves were compared using a Log-rank (Mantel-Cox) test. A one-way ANOVA was performed for both in vivo physiologic and histologic studies and in vitro studies at each terminal time point in experiments run in parallel. If significance was reached ($p<0.05$), a post-hoc all pairwise Multiple Comparison Procedures (Holm-Sidak method) was performed between each of the groups to determine significance. Prism 6 (GraphPad, La Jolla, CA) was used to statistically compare immunofluorescence between groups using a One-Way ANOVA (single staining) or Two-Way ANOVA (double staining). A Tukey's multiple comparisons test was performed post-hoc (One-Way ANOVA). Significance was defined as $p<0.05$.

Results

Based on initial studies demonstrating that MMI-0100 blocks MK2 to inhibit inflammation and fibrosis in non-cardiac disease models [5–7], we tested its utility in a model of acute myocardial infarction in vivo. Based on MK2's involvement in acute MI in genetic models of disease [12, 13], we hypothesized that MMI-0100 treatment, started at a clinically relevant 30 minutes post-LAD ligation, would modify the extracellular matrix changes that occur in AMI remodeling [26].

1.1 Treatment of acute myocardial infarction with MMI-0100 peptide protects cardiac function and attenuates dilation in vivo

To determine the effect of MMI-0100 on acute MI in vivo, three groups were investigated: 1) an acute myocardial infarction (AMI) experimental group; 2) an AMI experimental group given MMI-0100 thirty minutes after the completion of the permanent LAD occlusion at the previously established dose (50 μg/kg given daily [5], illustrated in Figure 1A); and 3) a

sham control group (receiving a thoracotomy and sham ligation). Baseline echocardiography was performed on each of the groups, followed by echocardiography at 7 and 14 days post-AMI to determine systolic cardiac function and size (Figure 1B). Two weeks after the permanent ligation of the LAD (AMI), ejection fraction decreased 26% and fractional shortening depressed 37% (Figure 1C, left column) compared to sham-operated control mice. Treatment of AMI with MMI-0100 reduced these loses in EF% and FS% to 12% and 20%, respectively (Figure 1C, left column). MMI-0100 similarly attenuated the increase in LV volume and LV end diastolic diameter (LVEDD) characteristic of AMI heart failure (Figure 1C, middle & right columns). Representative M-mode and 2-D video can be found in Figure 1D, Table 1 and online (1.2_WeeksShamSurgery, 2.2_Weeks_AMI, 3.2WeeksAMI_MMI-0100, respectively). Treatment of mice with MMI-0100 alone did not have any affect on cardiac function (Table 2) or survival (Supplemental Figure 1).

1.2 Treatment of acute MI with MMI-0100 treatment decreases cardiac fibrosis in vivo

Myocardial infarction triggers an inflammatory reaction that results in the formation of a scar. Healing from myocardial infarction is associated with alterations in the left ventricle, including dilation and hypertrophy [27]. In early stages of an acute MI, TGF-β has been proposed to play a role in deactivating macrophages and suppressing endothelial cell cytokine synthesis [27]. In later stages, TGF-β activates fibroblasts to deposit extracellular matrix (collagen) which contributes to left ventricular remodeling by promoting fibrosis in the non-infarcted myocardium, in addition to the myocardium directly affected by ischemia [27]. Consequences of this cardiac remodeling driven by TGF-β and fibrosis have been associated with myocardial stiffness and systolic and diastolic cardiac dysfunction, resulting in reduced cardiac output, heart failure and arrhythmias [28].

In our first studies, we identified that daily treatment with MMI-0100 preserved cardiac function and reduced the amount the heart dilated post-MI (Figure 1). We next investigated how MMI-0100 affected myocardial remodeling after acute MI by extensively analyzing the heart histologically for fibrosis in Masson's trichrome stained sections in a systemic manner (Figure 2A). Based on 4 hearts, analyzed blinded to treatment and objectively using computer algorithms recognizing fibrosis based on its hue, we demonstrated that mice subjected to AMI that then received MMI-0100 exhibited 50% less fibrosis than mice subjected to AMI alone (Figure 2B). These analyses, based on weighted averages of 168–180 cross sectional areas taken from the point of ligation all the way through the apex, demonstrated that the 20.6±2.2% fibrosis seen in AMI could be reduced to 11.1±2.2% fibrosis following treatment with MM1-0100 (Figure 2B). Since Masson's trichrome is a stain designed to detect collagen, which is present to a small extent in normal healthy hearts, we also performed analysis of the three control groups, including the thoracotomy and sham ligation, the no surgery and no drug group, and the group given daily MMI-0100 that did not undergo surgery. Extensive analysis of these hearts, paralleling methods used in the experimental groups, illustrated that collagen was present in less than 1% of the heart area (normal extracellular matrix and basement membranes) (Figure 2B). Taken together, these findings demonstrate that, in the setting of experimental AMI, MMI-0100 significantly reduces fibrosis response by 50% during the remodeling process, even when given 30 minutes after the ischemic insult.

With such a dramatic decrease in fibrosis, we next sought to characterize how this 50% decrease in fibrosis after AMI occurred in more detailed histological analysis. Representative histological sections from multiple individual hearts illustrated two general types of fibrosis sparing. First, fibrosis that occurred distant to the site of ischemia in AMI, illustrated in Figure 2C with arrows, was not found to the same extent in the heart sections treated with MMI-0100 (Figure 2D), although it was still present (see single arrow). The second observation was that fibrosis at the site of infarction after AMI was generally complete (all fibrotic), whereas when the MMI-0100 peptide was given, islands of viable myocytes (see asterisk, Figure 2D, top panel) could be identified. When investigated at a higher magnification, islands of myocyte sparing within the ischemic region scar were found routinely in hearts where MMI-0100 was given (Supplemental Figure 2D–F), in contrast to the complete fibrosis seen after AMI in all animals uniformly in multiple representative sections (Supplemental Figure 2A–C). Extent of sparing varied, being more localized to the endocardium at times (Supplemental Figure 2D, 2F, arrows), while being more transmural in others (Supplemental Figure 2E, see asterisk corresponding to asterisk in Figure 2D, top panel). These findings illustrate that MMI-0100's therapeutic benefit in the setting of AMI results in both critical muscle sparing at the site of ischemic insult, while at the same time reducing the distant non-ischemic site fibrosis that contributes to detrimental effects on cardiac function, consistent with functional findings in the same hearts (Figure 1). Given the mechanistic role of TGF-β in promoting fibrosis in non-infarcted myocardium, it is not surprising the MMI-0100's anti-TGF-β effect (via MK2 inhibition [5, 7]) reduced non-infarcted myocardial fibrosis, resulting in long-term protective effects on cardiac function.

1.3 MMI-0100 peptide post-hypoxia inhibits cardiomyocyte apoptosis in vitro by inhibiting MK2 activity

Our in vivo studies of AMI identified that MMI-0100 had an effect on both sparing cell death, including cardiomyocytes within the ischemic region itself, and in reducing non-infarcted myocardial fibrosis. Therefore, we next sought to determine underlying mechanisms by which MMI-0100 may afford cardiomyocytes and fibroblasts protection in these two processes. We first investigated how MMI-0100 affected cardiomyocytes by using cell lines derived from atrial (HL1) and ventricular (H9C2) cardiomyocytes, which have been established in models of acute myocardial infarction by culturing under anoxic (1% oxygen) conditions that induce cell death [29–33], at time points optimized in our hands. Activation of caspase 3/7 and LDH release were followed to monitor cell death in the presence of MMI-0100 at doses previously shown to suppress MK2 activity (20 and 100 μM) [5, 7].

When ventricular H9C2 myocyte-derived cells were challenged with 1% hypoxia (Figure 3A), caspase 3/7 activity increased <5 fold at 8 hours compared to cells harvested at the start of hypoxia challenge. At 16 and 24 hours, caspase 3/7 increased 15–20 fold (Figure 3B), paralleling increases in LDH release of 60–80% in the same cells (Figure 3C). The 100 μM MMI-0100 inhibited caspase 3/7 activity at 16 and 24 hours, suggesting that MMI-0100 inhibited apoptotic pathways at this time point (Figure 3B). Both 20 and 100 μM MMI-0100 significantly enhanced LDH release at 8 hours in cells challenged with 1% hypoxia, while only the 100 μM MMI-0100 concentration induced enhanced LDH release at 16 hours

(Figure 3B). Subsequent studies to determine the effect of MMI-0100 on LDH release in H9C2 cells in normoxic conditions demonstrated that MMI-0100 did not enhance LDH release in the absence of hypoxia at 8 hours (Supplemental Figure 3A). This confirms that MMI-0100 does not enhance LDH release directly, while parallel studies investigating MMI-0100 effects on the LDH assay itself found that MMI-0100 had no effect on the colorimetric assay itself (*data not shown*).

We next confirmed that the doses of MMI-0100 tested inhibited MK2 activity in the actual H9C2 cells tested in Figure 3. A recent study in mesothelial cells demonstrated that inhibiting MK2 activity with MMI-0100 reduced expression of downstream p-hnRNPA0 in response to fibrotic stimuli [5, 7]. Another study indicated that levels of total MK2 and p-MK2 protein were decreased [6]. Therefore, we investigated effects of MMI-0100 on hnRNPA0, total MK2, and p-MK2 at all time points tested in the caspase 3/7 activity and LDH release studies (Figure 4). 100 μM MMI-0100 significantly inhibited hnRNPA0 expression after being induced by hypoxia (Figure 4A), whereas total MK2 and p-MK2 protein levels were not changed significantly by MMI-0100 at either 20 or 100 μM MMI-0100 concentrations (Figure 4B).

When atrial HL1 myocyte-derived cells were challenged with 1% hypoxia (Figure 5A), caspase 3/7 activity increased 6 fold at 4 hours (Figure 5B). At 8 and 12 hours, caspase 3/7 activity increased ~10 fold (Figure 5B), paralleling increases in LDH release of 20–60% in the same cells (Figure 5C). 100 μM MMI-0100 inhibited caspase 3/7 activity at 12 hours, suggesting that MMI-0100 inhibited apoptotic pathways at this time point (Figure 5B). Both 20 and 100 μM MMI-0100 significantly enhanced LDH release at 4 hours in cells challenged with 1% hypoxia, while only 100 μM MMI-0100 enhanced LDH release at 8 hours (Figure 5C). Subsequent studies to determine the effect of MMI-0100 on LDH release of HL1 cells in normoxic conditions demonstrated that MMI-0100 did not enhance LDH release in the absence of hypoxia at 4 hours; unexpectedly, 100 μM MMI-0100 significantly inhibited LDH release (Supplemental Figure 3B).

We next confirmed that the doses of MMI-0100 tested inhibited MK2 activity in actual H9C2 cells tested in Figure 5. 100 μM MMI-0100 significantly inhibited hnRNPA0 expression at 4 and 8 hours after being induced by hypoxia (Figure 6A), whereas total MK2 and p-MK2 protein levels were not changed significantly by MMI-0100 peptide at either 20 or 100 μM MMI-0100 concentrations (Figure 6B). This confirms that MMI-0100 does not enhance LDH release directly.

1.4 MMI-0100 treatment post-hypoxia enhances primary cardiac fibroblast cell death in vitro despite inhibiting MK2 activity

Fibroblasts make up 70% of the cells in the heart [34, 35]; they are integral to repair of the heart, contributing to the remodeling process after ischemia, fibrosis and the progression of heart failure [36]. By physical and biochemical interaction with cardiomyocytes and the extracellular matrix, fibroblasts are positioned to sense and respond to injury. Since initial studies investigated MMI-0100's ability to inhibit fibrosis by inhibiting MK2 [6], we isolated primary cardiac fibroblasts as previously described in models of acute MI in culture [37–40], challenging them with 1% hypoxia in the presence or absence of MMI-0100 to

determine the peptide's effects on cell death. These studies were designed to parallel the cardiomyocyte studies (Supplemental Figure 3A), except with longer time points due to their relative resistance (compared to cardiomyocytes) to apoptosis (Supplemental Figure 3B) and LDH release (Supplemental Figure 3C). In contrast to the cardiomyocyte-derived cell lines described above, 100 μM MMI-0100 peptide treatment of cardiac fibroblasts significantly enhanced caspase 3/7 activity at 16 and 32 hours of hypoxia (Supplemental Figure 4B). LDH release was also significantly enhanced in cultured primary cardiac fibroblasts at 16, 32, and 48 hours of hypoxia (Supplemental Figure 3C). Subsequent studies to determine the effect of MMI-0100 on LDH release by primary cardiac fibroblasts in normoxic conditions demonstrated that MMI-0100 did not enhance LDH release in these cells in the absence of hypoxia at 4 hours (Supplemental Figure 4B). At the time points investigated, MMI-0100 did not change MK2 activity, as measured by hnRNPA0 protein levels by immunoblot at 16, 32, or 48 hours (Supplemental Figure 5A); similarly, protein levels of MK2 and p-MK2 did not significantly differ in the presence of MMI-0100 compared to hypoxia alone (Supplemental Figure 5B). Taken together, these studies suggest that MMI-0100 enhances cell death in the presence of hypoxia, and may suggest that decreased fibroblast viability is one mechanism by which treatment with MM1-0100 reduces fibrosis, leading to the decreased fibrosis seen in vivo (Figure 2).

1.5 MMI-0100 treatment reduces fibroblast number, increases arteriole density, and reduces cells with TGF-β1 in histological sections at two weeks post-AMI

The apparent decrease in fibroblasts (and presumably fibrosis), in addition to the inhibited cardiac cell death afforded cardiomyocytes when treated with MMI-0100 (Figure 3, Figure 4, Figure 5, Figure 6), represent two mechanisms by which MMI-0100 may improve cardiac function and attenuate cardiac dilation after AMI (Figure 1). To test this hypothesis, we returned to adjacent histological sections investigated above and quantified fibroblast numbers using anti-vimentin immunofluorescence (Figure 7A). Double-blinded non-biased computer analysis of the histological sections identified that MMI-0100 treatment resulted in a significant decrease in the number of vimentin-positive fibroblasts. Analysis of αSMA positive cells in these histological sections (Figure 7B) found that MMI-0100 given post-AMI also significantly increased the number of arterioles seen on cross-sectional analysis (also analyzed in a double-blinded non-biased manner)(Figure 7D).

Cardiac remodeling and fibrosis is driven by a number of factors, including release of TGF-β1. Since previous studies have demonstrated that MMI-0100 inhibits TGF-β1 secretion, we hypothesized that daily treatment with MMI-0100 during the post-AMI remodeling process would reduce TGF-β1 found histologically (Figure 8A). Blinded, non-biased quantitative analysis of TGF-β1 post-AMI by immunofluorescence confocal microscopy illustrated that MMI-0100 inhibited TGF-β1-positive cells by >50% (Figure 8B). In parallel, these adjacent histological sections had a significant reduction in TUNEL-positive cells, with a significant increase in the number of vimentin-positive cells (fibroblasts) that co-stained with TUNEL. Taken together, MMI-0100 treatment post-MI reduced the number of apoptotic cells histologically, while a greater number of primary fibroblasts underwent apoptosis in vivo, paralleling our findings of our in vitro studies.

Discussion

In the present study, we demonstrated for the first time the therapeutic benefit of cell-permeant peptide MK2 inhibitor, MMI-0100, when given 30 minutes after an acute myocardial infarction in vivo, followed by daily treatment. MMI-0100's cardioprotection includes a reduction in cardiac fibrosis and muscle sparing at two weeks. Functionally, MMI-0100 significantly preserves systolic function one week after MI, attenuating the rate at which systolic function is lost. Using two cardiomyocyte cell lines and primary cardiac fibroblast cell culture, we demonstrated that MMI-0100 inhibits MK2 to reduce cardiomyocyte caspase 3/7 activity, while enhancing primary cardiac fibroblast caspase 3/7 activity, which may explain MMI-0100's salvage of cardiac function and anti-fibrotic effects. Immunofluorescence analysis of fibroblast numbers and TGFβ1 positive cells in histological sections at two weeks post-MI supports these in vitro findings, suggesting that MMI-0100 decreases fibroblast numbers and TGFβ1 activity in vivo. These findings build upon MMI-0100's anti-inflammatory and anti-fibrotic properties shown in the settings of intimal hyperplasia associated with bypass surgery, bleomycin-induced pulmonary fibrosis, and post-surgical abdominal adhesions [5–7].

p38 MAPK activates (phosphorylates) MAPK Activated Protein Kinase-2 (MK2), to regulate ischemic injury in the heart. When mice lacking MK2 (MK2−/−) were compared to MK2 +/+ mice on a transgenic p38 background, transgenic p38-induced heart failure in MK2−/− mice was significantly protective [12]. Similarly, MK2−/− mice are resistant to ischemia reperfusion injury [13], implementing a critical role of MK2 in ischemic injury. Consistent with a MK2-p38 axis mediating ischemic cardiac damage, inhibiting p38 activation protects the heart against ischemic insult and cardiac dysfunction [41–45]. At the cellular level, ischemic activation of the MK2-p38 signaling pathway induces cardiac apoptosis [46], specifically in cardiomyocytes [9–11]. In fibroblasts, p38 regulates extracellular matrix proteins in primary cardiac fibroblasts during oxidative stress [47]. Consistent with a critical role for the MK2-p38 signaling axis, therapeutic inhibition of MK2 in the present studies was cardioprotective in vivo and resulted in decreased caspase 3/7 activity, which enhanced cell death (i.e. caspase 3/7 activity) in primary cardiac fibroblasts. While the blunt cell culture studies are helpful to delineate mechanistic insight into how MK2 inhibition may affect cell death in the complex microenvironment of the intact heart, the more detailed autocrine and paracrine effects of MK2 inhibition may be critical to understanding its mechanism(s) in the intact heart and may not be completely replicated in vitro.

MMI-0100 is a synthetic 22 amino acid cell-permeant peptide that enters cells to inhibit MAPKAP kinase 2 (MK2). The peptide inhibitor was derived from the heat shock protein b-1 consensus sequence for phosphorylation, and it inhibits the phosphorylation of HSPB1 at serine 86 by MK2 [48]. A cell-penetrating peptide (CPP) sequence was then added to this consensus sequence to facilitates its entry into cells to inhibit HSPB1 phosphorylation [7, 14, 49, 50]. Phase 1 human trials were begun in August 2014 in the Netherlands as a first-in-class inhibitor of MK2 to access safety, tolerability, and pharmacodynamics (http://www.drugdevelopment-technology.com/news/newsmoerae-matrix-begins-phase-i-trial-of-mmi-0100-treat-idiopathic-pulmonary-fibrosis-4336040). Pre-clinically, the drug has been

shown to attenuate fibrosis in idiopathic pulmonary fibrosis models and abdominal adhesions in vivo and to inhibit total MK2 levels [6] and HNRNPAO [7] in bleomycin-induced pulmonary fibrosis and abdominal adhesions, respectively. The cell types and temporal parameters of these studies differ in many ways compared to the present studies in isolated cardiac-derived cells and fibroblasts, which may explain the lack of demonstration of their MMI-0100's inhibition (MK2). Furthermore, signal transduction generally occurs over a small increment of time. Even with time course intervals as small as 4 hours, it is possible we either missed the inhibited time point or other yet-to-be-discovered signaling pathways in cardiomyocytes or cardiac fibroblasts were inhibited to results in the downstream inhibitory effects seen.

Peptides containing cell-penetrating domains, like MMI-0100, are taken up rapidly by cells and rapidly hydrolyzed in serum by peptidases. Despite this short serum half-life, the biologic effects of CPP-peptides are considerably longer, in the range of multiple days in several settings. The vasoactive CPP AZX100 prevents subarachnoid hemorrhage-induced vasospasm in a non-craniotomy rat model, observed typically 48 hours after the hemorrhage [51]. The cell-penetrating domain in AZX100 is identical to that found in the MMI-0100 peptide in the present studies. When fluorescently-tagged AZX100 is followed in cell culture in human fibroblasts, it can be identified for a week in culture [8]. This prolonged effect has been described for KAI-9803, a selective δ-PKC inhibitor (with a CPP) that comprises a peptidic fragment of the δ-PKC C2 domain (δ V1-1) conjugated by disulfide bond to a CPP (TAT47-57). Post-cerebral ischemia, KAI-9803 significantly reduces infarction size in the transient MCAO model, with effects maintained for at least seven days after administration [52]. The pharmacodynamics of MMI-0100 is similarly extended in a rat model of a jugular vein to carotid interposition graft. A single MMI-0100 dose (10^-6M for 20 minutes) at the time of explantation inhibits the development of intimal hyperplasia 28 days later [5].

A consistent finding in cardiomyocyte-derived cells (H9C2 and HL-1) and the primary cardiac fibroblast responses to hypoxia in vitro was that LDH release preceded the identification of apoptosis (specifically increased caspase-3/7 activity). The release of LDH from cells, reflecting the loss of cellular membrane integrity that occurs with cellular necrosis, has generally been shown to occur after the activation of caspases (e.g. caspase 3/7) that initiate apoptosis. For example, in adult cardiomyocytes, caspase activation occurs within the first few hours after the initiating stimuli, even if the ultrastructural changes and DNA fragmentation do not occur until many hours later (9+ hours) [53].

While MMI-0100 persists for some time in vivo, the point at which it is given is another important consideration. In the present study, we started MMI-0100 therapy 30 minutes after LAD ligation as a proof of concept. In the context of health delivery systems, this represent an optimistic time point in which heart attack might be able to receive therapy. Importantly, the processes that we initially were targeting were those that occur during the days and weeks after MI, involving fibroblasts and the remodeling process that occurs after ischemia, resulting in fibrosis and progression of heart failure [36]. By physical and biochemical interaction with cardiomyocytes and the extracellular matrix, fibroblasts are positioned to sense and respond rapidly to injury, uniquely aiding in repair after myocardial infarction [28,

54, 55]. So immediate inhibition may not be a therapeutic goal, given the way in which MMI-0100 targets fibroblasts post-MI. Importantly, it is the ongoing reactive fibrosis that occurs over weeks and months, characterized by increased extracellular matrix, that increases the likelihood of arrhythmias and sudden death [28]. Similarly, direct coupling of cardiomyocytes to myofibroblasts increases the likelihood of arrhythmias, in contrast to non-activated fibroblasts [56–58]. This reactive ongoing fibrosis leads to increased myocardial stiffness that contributes to systolic and diastolic dysfunction and heart failure progression [2, 59]. Beyond the unexpected effects of MMI-0100 on preventing cardiomyocyte apoptosis when given 30 minutes after AMI experimentally, the chronic late protective effects on fibroblasts likely do not depend on the rapid infusion (e.g. 30 minutes post-MI) of MMI-0100.

Interestingly, the inhibition of apoptosis using caspase inhibitors has been shown to result in enhanced necrosis [53]. In the present study, the enhanced necrosis seen with MMI-0100 corresponds with time points in which caspase-3/7 activity is inhibited, which may correspond to studies which illustrate that the caspase inhibition protecting cells from apoptosis results in increased levels of necrosis. This relationship is thought to be due to the perseverance of damaged mitochondria that do not apoptose (as the mitochondrial permeability transition is inhibited) [60]. The consequences of maintaining dysfunctional mitochondria is a bioenergetics catastrophe, culminating in the disruption of the plasma membrane, resulting in necrosis [60, 61], which may explain the divergent apoptosis and necrosis results MMI-0100 affords cardiomyocytes in the present study. The unexpected early LDH release and necrosis occurring before caspase-3/7 activation may have to do with the use of DMSO as vehicle, which has been reported to attenuate oxidative stress induced apoptosis via inhibiting p38 to exert a cardioprotective effects via regulation of heme oxygenase-1 [62, 63].

The mechanisms by which MMI-0100 protects against systolic dysfunction may be, in part, by its effects on inhibiting cytokine release. The role of MK2 in the innate immune system is well established [64], with MK2 inhibition suppressive the inflammatory responses in experimental arthritis [65, 66] and other autoimmune diseases [67]. Similarly, fibroblasts and cardiomyocytes can be considered to have innate immune responses, as hypoxia-induced inflammatory activation of p38 MAPK in cardiac fibroblasts, for example, stimulates the release of IL-1α, TNFα, and MMP-3 [68]. These cytokines can directly cardiomyocyte contractility depression, in addition to stimulating cardiomyocyte secretion of IL-1, IL-6, and TNFα. Since IL-1, IL-6, and TNFα all directly depress cardiac function and mediate heart failure [69], these non-cell death induced effects are critical to the dysfunction found in acute MI. In the present study, we investigated IL-1, IL6, and TNFα in the media of cardiomyocyte and primary cardiac fibroblasts at each of the time points tested. However, IL-1, IL6, and TNFα were undetectable (see Supplemental Table 1 and Supplemental Table 2). Either these cytokines were released and utilized much earlier than assayed, or this may be a limitation of using single cell suspensions that do not replicate the cross talk between cells (e.g. cardiomyocytes and fibroblasts) that occurs in vivo and plays an important role in cardiac function.

Anti-fibrosis strategies are limited and are not particularly targeted; currently, ACE inhibition, angiotensin receptor antagonism, and HMG-CoA-reductase inhibition are available [3, 70, 71]. While these have shown some beneficial effects (see Brown, et al., [72], more effective prevention focused at the level of the fibroblast is needed [73]. To this end, drugs that inhibit fibrosis more specifically are needed. Multiple anti-fibrotic agents have demonstrated potential therapeutic benefits in heart disease, including Perfenidone [74] and Transilast [75]. However, clinical utility of these compounds is limited by multiple undesirable side effects, including liver toxicity [76]. Novel anti-fibrotic agents based on the core structure of Transilast (FT011) have subsequently been approved for pre-clinical development of diabetic nephropathy and have been tested for treatment of experimental diabetic cardiomyopathy [77, 78]. Use of relaxin to reduce fibrosis post-AMI has been reported [79] and use of recombinant relaxin in Phase 2 and Phase 3 clinical of acute heart failure and decompensated congestive heart failure have been completed, with results in process [80–82].

Conclusion

Therapeutic inhibition of Mitogen Activated Protein Kinase Activated Protein Kinase II (MK2) activity using rationally designed cell-permeant peptides after acute MI inhibits cardiac fibrosis and retains cardiac function at 2 weeks, by mechanisms that involve inhibiting cardiomyocyte apoptosis, while enhancing primary cardiac fibroblast cell death.

Supplementary Material

Refer to Web version on PubMed Central for supplementary material.

Acknowledgments

The authors wish to thank Caryn Peterson and Alyssa Panitch for their guidance using MMI-0100 in cell culture and for and monitoring MK2 activity in vitro; Brian Jensen and Wei Huang for their assistance with primary cardiac fibroblasts isolation; Janice Weaver (University of North Carolina-Lineberger Center Animal Histopathology Laboratory) for her extensive consultation and preparation of the histological specimens; and Dr. Mauricio Rojas in the McAllister Heart Rodent Advanced Surgical Models Core Lab for his assistance with the surgeries. We also thank Dr. William Claycomb for the HL-1 cells used in this study, and Dr. David Barrow in the UNC Cytokine and Biomarker Analysis Facility for his technical assistance with the cytokine assays. This work was supported by the National Institutes of Health (R01HL104129 to M.W.), a Fellowship from the Jefferson-Pilot Corporation (to M.W.), and the Fondation Leducq (to C.P. and M.W.).

Glossary

AMI	Acute myocardial infarction
LAD	Left anterior descending
MK2	Mitogen Activated Protein Kinase Activated Protein Kinase II
MMI-0100	cell permeant peptide inhibitor of MK2 activity
PBS	phosphate buffered saline
TGF-β	transforming growth factor beta

References

1. Roger VL, Go AS, Lloyd-Jones DM, Benjamin EJ, Berry JD, Borden WB, et al. Executive summary: heart disease and stroke statistics--2012 update: a report from the American Heart Association. Circulation. 2012; 125:188–97. [PubMed: 22215894]
2. Pfeffer MA, Braunwald E. Ventricular remodeling after myocardial infarction. Experimental observations and clinical implications. Circulation. 1990; 81:1161–72. [PubMed: 2138525]
3. Opie LH, Commerford PJ, Gersh BJ, Pfeffer MA. Controversies in ventricular remodelling. Lancet. 2006; 367:356–67. [PubMed: 16443044]
4. Dorn GW 2nd. Novel pharmacotherapies to abrogate postinfarction ventricular remodeling. Nat Rev Cardiol. 2009; 6:283–91. [PubMed: 19352332]
5. Muto A, Panitch A, Kim N, Park K, Komalavilas P, Brophy CM, et al. Inhibition of Mitogen Activated Protein Kinase Activated Protein Kinase II with MMI-0100 reduces intimal hyperplasia ex vivo and in vivo. Vascular pharmacology. 2012; 56:47–55. [PubMed: 22024359]
6. Vittal R, Fisher A, Gu H, Mickler EA, Panitch A, Lander C, et al. Peptide-mediated Inhibition of MK2 Ameliorates Bleomycin-Induced Pulmonary Fibrosis. Am J Respir Cell Mol Biol. 2013
7. Ward BC, Kavalukas S, Brugnano J, Barbul A, Panitch A. Peptide inhibitors of MK2 show promise for inhibition of abdominal adhesions. The Journal of surgical research. 2011; 169:e27–36. [PubMed: 21492875]
8. Flynn CR, Cheung-Flynn J, Smoke CC, Lowry D, Roberson R, Sheller MR, et al. Internalization and intracellular trafficking of a PTD-conjugated anti-fibrotic peptide, AZX100, in human dermal keloid fibroblasts. Journal of pharmaceutical sciences. 2010; 99:3100–21. [PubMed: 20140957]
9. Clark JE, Sarafraz N, Marber MS. Potential of p38-MAPK inhibitors in the treatment of ischaemic heart disease. Pharmacol Ther. 2007; 116:192–206. [PubMed: 17765316]
10. Kerkela R, Force T. p38 mitogen-activated protein kinase: a future target for heart failure therapy? Journal of the American College of Cardiology. 2006; 48:556–8. [PubMed: 16875983]
11. Wang Y. Mitogen-activated protein kinases in heart development and diseases. Circulation. 2007; 116:1413–23. [PubMed: 17875982]
12. Streicher, JM. The role of mitogen activated protein kinase activated protein kinase-2 in regulating p38 mitogen activated protein kinase induced cyclooxygenase-2 induction and heart failure. University of California; Los Angelos: 2009.
13. Shiroto K, Otani H, Yamamoto F, Huang CK, Maulik N, Das DK. MK2−/− gene knockout mouse hearts carry anti-apoptotic signal and are resistant to ischemia reperfusion injury. Journal of molecular and cellular cardiology. 2005; 38:93–7. [PubMed: 15623425]
14. Ward B, Seal BL, Brophy CM, Panitch A. Design of a bioactive cell-penetrating peptide: when a transduction domain does more than transduce. Journal of peptide science : an official publication of the European Peptide Society. 2009; 15:668–74. [PubMed: 19691016]
15. Maejima Y, Kyoi S, Zhai P, Liu T, Li H, Ivessa A, et al. Mst1 inhibits autophagy by promoting the interaction between Beclin1 and Bcl-2. Nature medicine. 2013; 19:1478–88.
16. Qian L, Huang Y, Spencer CI, Foley A, Vedantham V, Liu L, et al. In vivo reprogramming of murine cardiac fibroblasts into induced cardiomyocytes. Nature. 2012; 485:593–8. [PubMed: 22522929]
17. Oakley RH, Ren R, Cruz-Topete D, Bird GS, Myers PH, Boyle MC, et al. Essential role of stress hormone signaling in cardiomyocytes for the prevention of heart disease. Proceedings of the National Academy of Sciences of the United States of America. 2013; 110:17035–40. [PubMed: 24082121]
18. Willis MS, Homeister JW, Rosson GB, Annayev Y, Holley D, Holly SP, et al. Functional redundancy of SWI/SNF catalytic subunits in maintaining vascular endothelial cells in the adult heart. Circulation research. 2012; 111:e111–22. [PubMed: 22740088]
19. Willis MS, Schisler JC, Li L, Rodriguez JE, Hilliard EG, Charles PC, et al. Cardiac muscle ring finger-1 increases susceptibility to heart failure in vivo. Circulation research. 2009; 105:80–8. [PubMed: 19498199]
20. Santiago JJ, Dangerfield AL, Rattan SG, Bathe KL, Cunnington RH, Raizman JE, et al. Cardiac fibroblast to myofibroblast differentiation in vivo and in vitro: expression of focal adhesion

components in neonatal and adult rat ventricular myofibroblasts. Developmental dynamics : an official publication of the American Association of Anatomists. 2010; 239:1573–84. [PubMed: 20503355]

21. Yates CC, Krishna P, Whaley D, Bodnar R, Turner T, Wells A. Lack of CXC chemokine receptor 3 signaling leads to hypertrophic and hypercellular scarring. The American journal of pathology. 2010; 176:1743–55. [PubMed: 20203286]
22. Claycomb WC, Lanson NA Jr, Stallworth BS, Egeland DB, Delcarpio JB, Bahinski A, et al. HL-1 cells: a cardiac muscle cell line that contracts and retains phenotypic characteristics of the adult cardiomyocyte. Proceedings of the National Academy of Sciences of the United States of America. 1998; 95:2979–84. [PubMed: 9501201]
23. White SM, Constantin PE, Claycomb WC. Cardiac physiology at the cellular level: use of cultured HL-1 cardiomyocytes for studies of cardiac muscle cell structure and function. American journal of physiology Heart and circulatory physiology. 2004; 286:H823–9. [PubMed: 14766671]
24. Toraason M, Luken ME, Breitenstein M, Krueger JA, Biagini RE. Comparative toxicity of allylamine and acrolein in cultured myocytes and fibroblasts from neonatal rat heart. Toxicology. 1989; 56:107–17. [PubMed: 2728003]
25. LaFramboise WA, Scalise D, Stoodley P, Graner SR, Guthrie RD, Magovern JA, et al. Cardiac fibroblasts influence cardiomyocyte phenotype in vitro. American journal of physiology Cell physiology. 2007; 292:C1799–808. [PubMed: 17229813]
26. Agnoletti G, Cargnoni A, Agnoletti L, Di Marcello M, Balzarini P, Pasini E, et al. Experimental ischemic cardiomyopathy: insights into remodeling, physiological adaptation, and humoral response. Annals of clinical and laboratory science. 2006; 36:333–40. [PubMed: 16951276]
27. Bujak M, Frangogiannis NG. The role of TGF-beta signaling in myocardial infarction and cardiac remodeling. Cardiovascular research. 2007; 74:184–95. [PubMed: 17109837]
28. van den Borne SW, Diez J, Blankesteijn WM, Verjans J, Hofstra L, Narula J. Myocardial remodeling after infarction: the role of myofibroblasts. Nat Rev Cardiol. 2010; 7:30–7. [PubMed: 19949426]
29. Sun J, Sun G, Meng X, Wang H, Wang M, Qin M, et al. Ginsenoside RK3 Prevents Hypoxia-Reoxygenation Induced Apoptosis in H9c2 Cardiomyocytes via AKT and MAPK Pathway. Evidence-based complementary and alternative medicine : eCAM. 2013; 2013:690190. [PubMed: 23935671]
30. Zhang C, Lin G, Wan W, Li X, Zeng B, Yang B, et al. Resveratrol, a polyphenol phytoalexin, protects cardiomyocytes against anoxia/reoxygenation injury via the TLR4/NF-kappaB signaling pathway. International journal of molecular medicine. 2012; 29:557–63. [PubMed: 22246136]
31. Bukowska A, Hammwohner M, Sixdorf A, Schild L, Wiswedel I, Rohl FW, et al. Dronedarone prevents microcirculatory abnormalities in the left ventricle during atrial tachypacing in pigs. British journal of pharmacology. 2012; 166:964–80. [PubMed: 22103242]
32. Liu SX, Zhang Y, Wang YF, Li XC, Xiang MX, Bian C, et al. Upregulation of heme oxygenase-1 expression by hydroxysafflor yellow A conferring protection from anoxia/reoxygenation-induced apoptosis in H9c2 cardiomyocytes. International journal of cardiology. 2012; 160:95–101. [PubMed: 21497407]
33. Severino A, Campioni M, Straino S, Salloum FN, Schmidt N, Herbrand U, et al. Identification of protein disulfide isomerase as a cardiomyocyte survival factor in ischemic cardiomyopathy. Journal of the American College of Cardiology. 2007; 50:1029–37. [PubMed: 17825711]
34. Jugdutt BI. Ventricular remodeling after infarction and the extracellular collagen matrix: when is enough enough? Circulation. 2003; 108:1395–403. [PubMed: 12975244]
35. Banerjee I, Fuseler JW, Price RL, Borg TK, Baudino TA. Determination of cell types and numbers during cardiac development in the neonatal and adult rat and mouse. American journal of physiology Heart and circulatory physiology. 2007; 293:H1883–91. [PubMed: 17604329]
36. Porter KE, Turner NA. Cardiac fibroblasts: at the heart of myocardial remodeling. Pharmacol Ther. 2009; 123:255–78. [PubMed: 19460403]
37. Rupp H, Maisch B. Control of apoptosis of cardiovascular fibroblasts: a novel drug target. Herz. 1999; 24:225–31. [PubMed: 10412646]

38. Sangeetha M, Pillai MS, Philip L, Lakatta EG, Shivakumar K. NF-kappaB inhibition compromises cardiac fibroblast viability under hypoxia. Experimental cell research. 2011; 317:899–909. [PubMed: 21211536]
39. Chu W, Li X, Li C, Wan L, Shi H, Song X, et al. TGFBR3, a potential negative regulator of TGF-beta signaling, protects cardiac fibroblasts from hypoxia-induced apoptosis. Journal of cellular physiology. 2011; 226:2586–94. [PubMed: 21792916]
40. Leicht M, Briest W, Holzl A, Zimmer HG. Serum depletion induces cell loss of rat cardiac fibroblasts and increased expression of extracellular matrix proteins in surviving cells. Cardiovascular research. 2001; 52:429–37. [PubMed: 11738059]
41. Marber MS, Rose B, Wang Y. The p38 mitogen-activated protein kinase pathway--a potential target for intervention in infarction, hypertrophy, and heart failure. Journal of molecular and cellular cardiology. 2011; 51:485–90. [PubMed: 21062627]
42. Tanno M, Bassi R, Gorog DA, Saurin AT, Jiang J, Heads RJ, et al. Diverse mechanisms of myocardial p38 mitogen-activated protein kinase activation: evidence for MKK-independent activation by a TAB1-associated mechanism contributing to injury during myocardial ischemia. Circulation research. 2003; 93:254–61. [PubMed: 12829618]
43. Marais E, Genade S, Huisamen B, Strijdom JG, Moolman JA, Lochner A. Activation of p38 MAPK induced by a multi-cycle ischaemic preconditioning protocol is associated with attenuated p38 MAPK activity during sustained ischaemia and reperfusion. Journal of molecular and cellular cardiology. 2001; 33:769–78. [PubMed: 11273729]
44. Sanada S, Kitakaze M, Papst PJ, Hatanaka K, Asanuma H, Aki T, et al. Role of phasic dynamism of p38 mitogen-activated protein kinase activation in ischemic preconditioning of the canine heart. Circulation research. 2001; 88:175–80. [PubMed: 11157669]
45. Nagarkatti DS, Sha'afi RI. Role of p38 MAP kinase in myocardial stress. Journal of molecular and cellular cardiology. 1998; 30:1651–64. [PubMed: 9841266]
46. Matsumoto-Ida M, Takimoto Y, Aoyama T, Akao M, Takeda T, Kita T. Activation of TGF-beta1-TAK1-p38 MAPK pathway in spared cardiomyocytes is involved in left ventricular remodeling after myocardial infarction in rats. American journal of physiology Heart and circulatory physiology. 2006; 290:H709–15. [PubMed: 16183734]
47. Hsu PL, Su BC, Kuok QY, Mo FE. Extracellular matrix protein CCN1 regulates cardiomyocyte apoptosis in mice with stress-induced cardiac injury. Cardiovascular research. 2013; 98:64–72. [PubMed: 23329650]
48. Hayess K, Benndorf R. Effect of protein kinase inhibitors on activity of mammalian small heat-shock protein (HSP25) kinase. Biochemical pharmacology. 1997; 53:1239–47. [PubMed: 9214684]
49. Lopes LB, Flynn C, Komalavilas P, Panitch A, Brophy CM, Seal BL. Inhibition of HSP27 phosphorylation by a cell-permeant MAPKAP Kinase 2 inhibitor. Biochemical and biophysical research communications. 2009; 382:535–9. [PubMed: 19289101]
50. Ho A, Schwarze SR, Mermelstein SJ, Waksman G, Dowdy SF. Synthetic protein transduction domains: enhanced transduction potential in vitro and in vivo. Cancer research. 2001; 61:474–7. [PubMed: 11212234]
51. Furnish EJ, Brophy CM, Harris VA, Macomson S, Winger J, Head GA, et al. Treatment with transducible phosphopeptide analogues of the small heat shock-related protein, HSP20, after experimental subarachnoid hemorrhage: prevention and reversal of delayed decreases in cerebral perfusion. Journal of neurosurgery. 2010; 112:631–9. [PubMed: 20192670]
52. Sho, E.; Dong, J.; Jin, Z.; Begley, R.; Chen, L.; Harrison, SD., et al. Protein kinase C-δ inhibitor protects against ischemic stroke by inhibiting cellular injury and inflammation and promoting astrocyte proliferation. International Stroke Conference; 2008; p. 671-2.
53. Suzuki K, Kostin S, Person V, Elsasser A, Schaper J. Time course of the apoptotic cascade and effects of caspase inhibitors in adult rat ventricular cardiomyocytes. Journal of molecular and cellular cardiology. 2001; 33:983–94. [PubMed: 11343420]
54. Hinz B, Phan SH, Thannickal VJ, Prunotto M, Desmouliere A, Varga J, et al. Recent developments in myofibroblast biology: paradigms for connective tissue remodeling. The American journal of pathology. 2012; 180:1340–55. [PubMed: 22387320]

55. Tomasek JJ, Gabbiani G, Hinz B, Chaponnier C, Brown RA. Myofibroblasts and mechano-regulation of connective tissue remodelling. Nat Rev Mol Cell Biol. 2002; 3:349–63. [PubMed: 11988769]
56. Rohr S. Myofibroblasts in diseased hearts: new players in cardiac arrhythmias? Heart Rhythm. 2009; 6:848–56. [PubMed: 19467515]
57. Thompson SA, Copeland CR, Reich DH, Tung L. Mechanical coupling between myofibroblasts and cardiomyocytes slows electric conduction in fibrotic cell monolayers. Circulation. 2011; 123:2083–93. [PubMed: 21537003]
58. Rosker C, Salvarani N, Schmutz S, Grand T, Rohr S. Abolishing myofibroblast arrhythmogeneicity by pharmacological ablation of alpha-smooth muscle actin containing stress fibers. Circulation research. 2011; 109:1120–31. [PubMed: 21921266]
59. Swynghedauw B. Molecular mechanisms of myocardial remodeling. Physiol Rev. 1999; 79:215–62. [PubMed: 9922372]
60. Kroemer G, Dallaporta B, Resche-Rigon M. The mitochondrial death/life regulator in apoptosis and necrosis. Annual review of physiology. 1998; 60:619–42.
61. Hirsch T, Marchetti P, Susin SA, Dallaporta B, Zamzami N, Marzo I, et al. The apoptosis-necrosis paradox. Apoptogenic proteases activated after mitochondrial permeability transition determine the mode of cell death. Oncogene. 1997; 15:1573–81. [PubMed: 9380409]
62. Man W, Ming D, Fang D, Chao L, Jing C. Dimethyl sulfoxide attenuates hydrogen peroxide-induced injury in cardiomyocytes via heme oxygenase-1. Journal of cellular biochemistry. 2014; 115:1159–65. [PubMed: 24415199]
63. Chen XQ, Wu SH, Zhou Y, Tang YR. Lipoxin A4-induced heme oxygenase–1 protects cardiomyocytes against hypoxia/reoxygenation injury via p38 MAPK activation and Nrf2/ARE complex. PloS one. 2013; 8:e67120. [PubMed: 23826208]
64. Adams V, Mangner N, Gasch A, Krohne C, Gielen S, Hirner S, et al. Induction of MuRF1 is essential for TNF-alpha-induced loss of muscle function in mice. J Mol Biol. 2008; 384:48–59. [PubMed: 18804115]
65. Hegen M, Gaestel M, Nickerson-Nutter CL, Lin LL, Telliez JB. MAPKAP kinase 2-deficient mice are resistant to collagen-induced arthritis. Journal of immunology. 2006; 177:1913–7.
66. Mourey RJ, Burnette BL, Brustkern SJ, Daniels JS, Hirsch JL, Hood WF, et al. A benzothiophene inhibitor of mitogen-activated protein kinase-activated protein kinase 2 inhibits tumor necrosis factor alpha production and has oral anti-inflammatory efficacy in acute and chronic models of inflammation. The Journal of pharmacology and experimental therapeutics. 2010; 333:797–807. [PubMed: 20237073]
67. Thiel MJ, Schaefer CJ, Lesch ME, Mobley JL, Dudley DT, Tecle H, et al. Central role of the MEK/ERK MAP kinase pathway in a mouse model of rheumatoid arthritis: potential proinflammatory mechanisms. Arthritis and rheumatism. 2007; 56:3347–57. [PubMed: 17907188]
68. Tondera C, Laube M, Wimmer C, Kniess T, Mosch B, Grossmann K, et al. Visualization of cyclooxygenase-2 using a 2,3-diarylsubstituted indole-based inhibitor and confocal laser induced cryofluorescence microscopy at 20K in melanoma cells in vitro. Biochemical and biophysical research communications. 2013; 430:301–6. [PubMed: 23146632]
69. El-Menyar AA. Cytokines and myocardial dysfunction: state of the art. J Card Fail. 2008; 14:61–74. [PubMed: 18226775]
70. Bauersachs J, Galuppo P, Fraccarollo D, Christ M, Ertl G. Improvement of left ventricular remodeling and function by hydroxymethylglutaryl coenzyme a reductase inhibition with cerivastatin in rats with heart failure after myocardial infarction. Circulation. 2001; 104:982–5. [PubMed: 11524389]
71. Shyu KG, Wang BW, Chen WJ, Kuan P, Hung CR. Mechanism of the inhibitory effect of atorvastatin on endoglin expression induced by transforming growth factor-beta1 in cultured cardiac fibroblasts. Eur J Heart Fail. 2010; 12:219–26. [PubMed: 20156938]
72. Brown RD, Ambler SK, Mitchell MD, Long CS. The cardiac fibroblast: therapeutic target in myocardial remodeling and failure. Annu Rev Pharmacol Toxicol. 2005; 45:657–87. [PubMed: 15822192]

73. Fraccarollo D, Galuppo P, Bauersachs J. Novel therapeutic approaches to post-infarction remodelling. Cardiovascular research. 2012; 94:293–303. [PubMed: 22387461]

74. Lee KW, Everett THt, Rahmutula D, Guerra JM, Wilson E, Ding C, et al. Pirfenidone prevents the development of a vulnerable substrate for atrial fibrillation in a canine model of heart failure. Circulation. 2006; 114:1703–12. [PubMed: 17030685]

75. Martin J, Kelly DJ, Mifsud SA, Zhang Y, Cox AJ, See F, et al. Tranilast attenuates cardiac matrix deposition in experimental diabetes: role of transforming growth factor-beta. Cardiovascular research. 2005; 65:694–701. [PubMed: 15664396]

76. Holmes DR Jr, Savage M, LaBlanche JM, Grip L, Serruys PW, Fitzgerald P, et al. Results of Prevention of REStenosis with Tranilast and its Outcomes (PRESTO) trial. Circulation. 2002; 106:1243–50. [PubMed: 12208800]

77. Zhang Y, Edgley AJ, Cox AJ, Powell AK, Wang B, Kompa AR, et al. FT011, a new anti-fibrotic drug, attenuates fibrosis and chronic heart failure in experimental diabetic cardiomyopathy. Eur J Heart Fail. 2012; 14:549–62. [PubMed: 22417655]

78. Zammit SC, Cox AJ, Gow RM, Zhang Y, Gilbert RE, Krum H, et al. Evaluation and optimization of antifibrotic activity of cinnamoyl anthranilates. Bioorg Med Chem Lett. 2009; 19:7003–6. [PubMed: 19879136]

79. Samuel CS, Cendrawan S, Gao XM, Ming Z, Zhao C, Kiriazis H, et al. Relaxin remodels fibrotic healing following myocardial infarction. Laboratory investigation; a journal of technical methods and pathology. 2011; 91:675–90.

80. Miyares MA, Davis KA. Serelaxin, a ‘breakthrough’ investigational intravenous agent for acute heart failure. P & T : a peer-reviewed journal for formulary management. 2013; 38:606–11. [PubMed: 24391379]

81. Du XJ, Hewitson TD, Nguyen MN, Samuel CS. Therapeutic effects of serelaxin in acute heart failure. Circulation journal : official journal of the Japanese Circulation Society. 2014; 78:542–52. [PubMed: 24451687]

82. Cotter G, Milo O, Davison BA. Increased Mortality after an Acute Heart Failure Episode: New Pathophysiological Insights from the RELAX-AHF Study and Beyond. Current heart failure reports. 2014; 11:19–30. [PubMed: 24363020]

Highlights

- MK2 −/− mice are resistant to ischemia reperfusion injury
- MMI-0100 is a cell-permeable peptide inhibitor of MK2 that prevents lung fibrosis
- MMI-0100 therapy after LAD ligation reduces fibrosis ~50% and protects function
- MMI-0100 inhibits MK2 to reduce ischemia-induced cardiomyocyte apoptosis
- MMI-0100 enhances ischemia-induced fibroblast apoptosis to provide anti-fibrosis

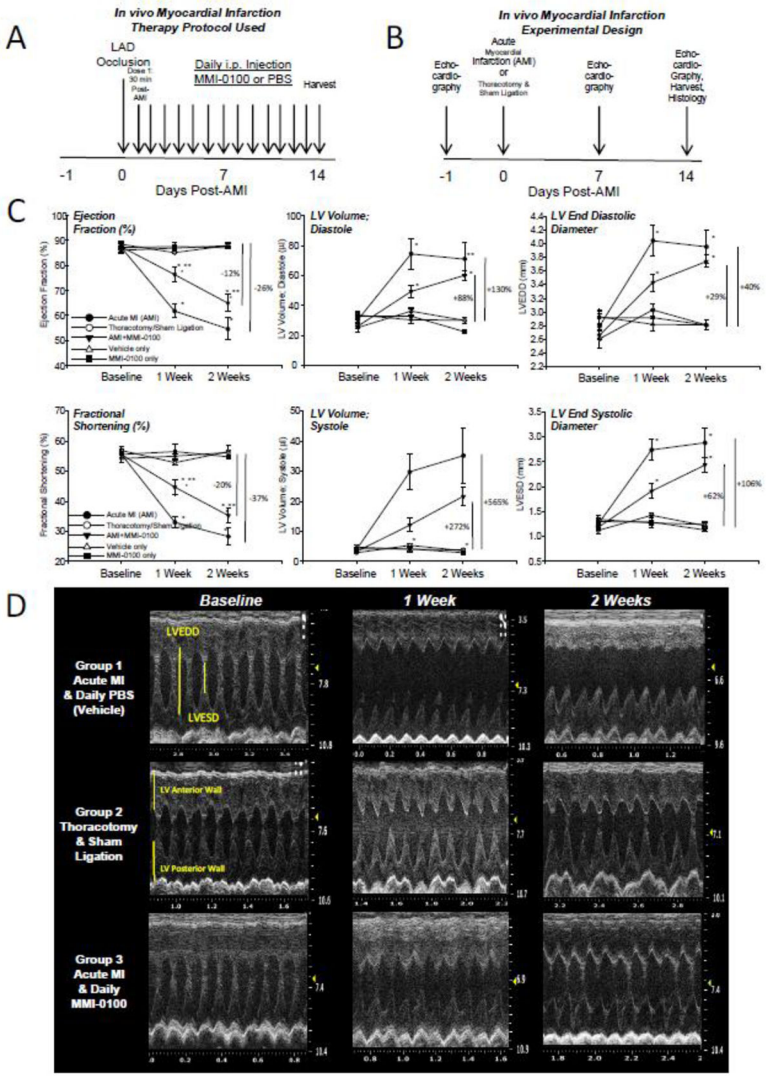

Figure 1.

Experimental design of acute myocardial infarction (AMI) with 50 μg/kg/day MMI-0100 peptide or PBS intraperitoneal treatment given 30 minutes after insults with survival analysis. **A.** Echocardiography schedule in relation to acute myocardial infarction (AMI) and thoracotomy and sham ligation surgical intervention. **B.** Daily drug delivery schedule of MMI-0100 peptide or PBS control. **C.** Conscious echocardiographic analysis of AMI (thoracotomy and permanent LAD coronary artery ligation), thoracotomy and sham ligation (threaded, but not tied, removed), and AMI followed by intraperitoneal MMI-0100 peptide in PBS vehicle, started 30 minutes AFTER permanent LAD ligation placed. **D.** Representative M-mode tracing from three experimental groups at baseline, 1 week, and 2 weeks after AMI surgical intervention. LVEDD, left ventricular end-diastolic dimension; LVESD, left ventricular end-systolic dimension; LV Vol;d, LV volume in diastole; LV Vol;s,, LV volume in systole; FS, fractional shortening, calculated as (LVEDD-LVESD)/ LVEDD × 100; EF%, ejection fraction calculated as (end Simpson's diastolic volume – end Simpson's systolic volume)/end Simpson's diastolic volume * 100. A Kruskal-Wallis One-

way ANOVA was performed at each terminal time point in experiments setup and ran in parallel. If significance was reached ($p<0.05$), a post-hoc all pairwise Multiple Comparison Procedures (Tukey Test) was performed between each of the groups to determine significance. *$p<0.05$ vs. thoracotomy and sham ligation (control); **$p<0.05$ vs. other two groups. Image in A from: http://www.clipartbest.com/clipart-RTA6ngxgc

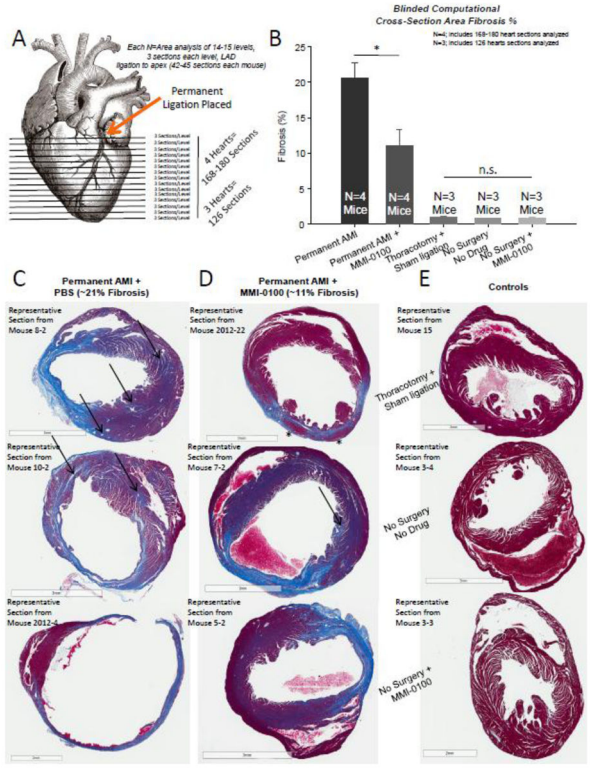

Figure 2.

After surgical induction of acute MI (permanent LAD coronary artery ligation), daily treatment with 50 μg/kg/day MMI-0100 peptide (first given 30 minutes post-AMI) in vivo results in a significant reduction in fibrosis at day 14. **A.** The area of fibrosis was analyzed in 3–4 blindly chosen hearts each heart at 14–15 levels, 3 sections at each level, and analyzed blinded fibrosis analysis of trichrome stained histological sections using Aperio (42 sections analyzed per mouse heart). **B.** Histological analysis of fibrosis (collagen staining blue by Aperio algorithm analysis) of 3–4 hearts per group resulting from acute myocardial infarction at 14 days post-AMI. **C.** Representative trichrome-stained sections from mouse hearts challenged with permanent AMI (~21% of the area stains blue, including primarily interstitial fibrosis). **D.** Representative trichrome-stained sections from mouse hearts challenged with permanent AMI treated daily with 50 μg/kg/day MMI-0100 peptide starting 30 minutes post-infarction (~11% of the area stains blue, including primarily interstitial fibrosis). **E.** Representative trichrome-stained sections from mouse control hearts, including the thoracotomy + sham ligation, no surgery + no drug, and no surgery+50 μg/kg/day MMI-0100 peptide. (0.9% of the area stains blue, representing connective tissue and vessels; no interstitial fibrosis evident in any analyzed section). A Kruskal-Wallis One-way ANOVA was performed on the fibrosis % from serial sections using 3–4 hearts per group; each single fibrosis per heart was the weighted mean of 126–180 sections described in **A.** above. If significance was reached ($p<0.05$), a post-hoc all pairwise Multiple Comparison Procedures (Tukey Test) was performed between each of the groups to determine significance. *$p<0.05$ vs. all other groups.

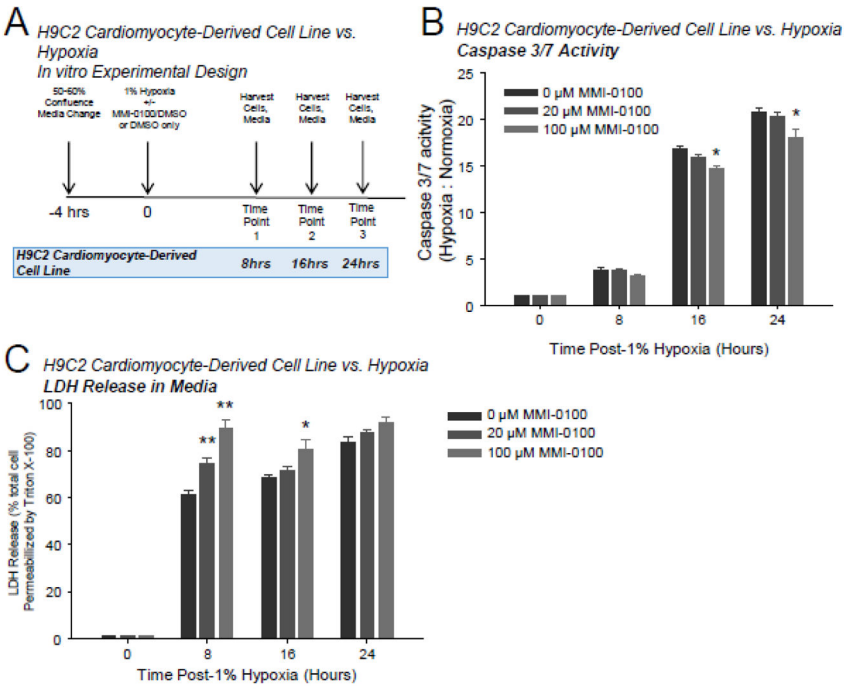

Figure 3.

In H9C2 cardiomyocytes challenged with 1% hypoxia, MMI-0100 peptide reduces caspase 3/7 activation. **A.** H9C2 cells were challenged with 1% hypoxia for 8, 16, and 24 hours; the media was collected for LDH release and cells immediately harvested for caspase 3/7 activity and Western blot analysis at each time point. Each bar represents 3 wells performed in triplicate in experimental conditions repeated on at least 2 independent occasions. **B.** Caspase 3/7 activity of harvested cells at 8, 16, and 24 hours in the presence or absence of MMI-0100 peptide; 0 µM (vehicle only, 0.1% DMSO final), 20 µM, or 100 µM MMI-0100 peptide. **C.** LDH detection in media from the same experimental conditions as the caspase activity described above. A Kruskal-Wallis One-way ANOVA was performed at each terminal time point in experiments setup and ran in parallel. If significance was reached ($p<0.05$), a post-hoc all pairwise Multiple Comparison Procedures (Tukey Test) was performed between each of the groups to determine significance. *$p<0.05$ vs. 0 µM group (DMSO vehicle control); **$p<0.05$ vs. other two groups.

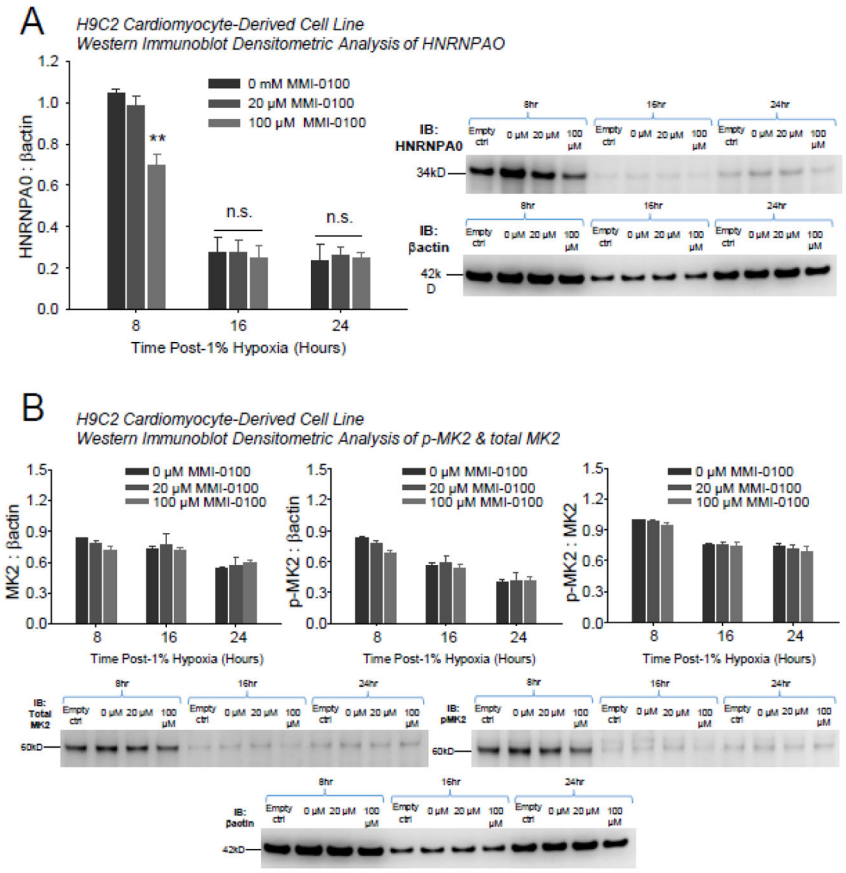

Figure 4.

In H9C2 cardiomyocytes challenged with 1% hypoxia, MMI-0100 peptide reduces MK2 activity measured by downstream HNRNPA0 protein expressed, but not phospho- or total MK2 levels. A. H9C2 cells were challenged with 1% hypoxia for 8, 16, and 24 hours; desitometric analysis of Western immunoblot (right, representative 1 of 3 replicates per bar) demonstrated significant decreases in HNRNPA0 protein expression. B. Densitometric analysis phospho- and total MK2 levels (below). A Kruskal-Wallis One-way ANOVA was performed at each terminal time point in experiments setup and ran in parallel. If significance was reached ($p<0.05$), a post-hoc all pairwise Multiple Comparison Procedures (Tukey Test) was performed between each of the groups to determine significance. **$p<0.05$ vs. other 2 groups.

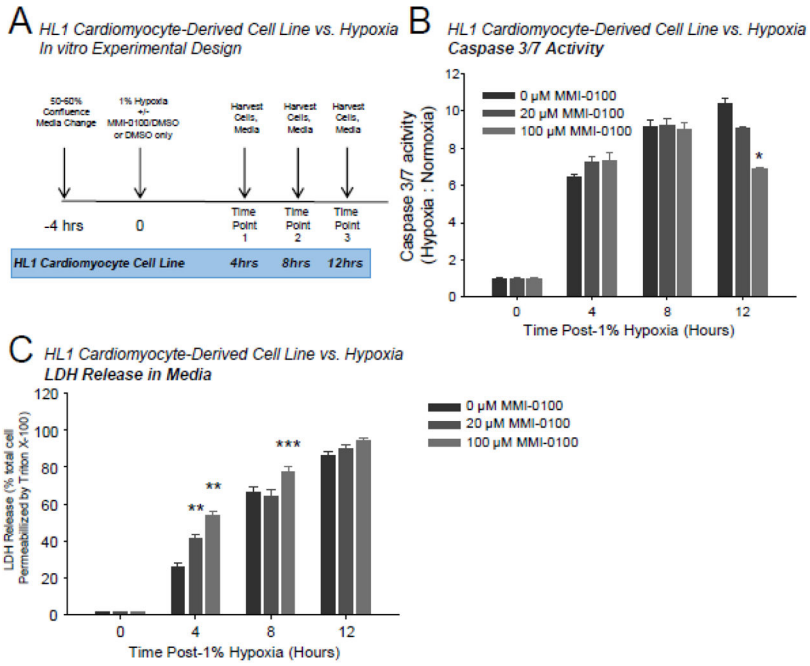

Figure 5.

In HL1 cardiomyocytes challenged with 1% hypoxia, MMI-0100 peptide reduces caspase 3/7 activation. **A.** HL1 cells were challenged with 1% hypoxia for 4, 8, and 12 hours; the media was collected for LDH release and cells immediately harvested for caspase 3/7 activity and Western blot analysis at each time point. Each bar represents 3 wells performed in triplicate in experimental conditions repeated on at least 2 independent occasions. **B.** Caspase 3/7 activity of harvested cells at 4, 8, and 12 hours in the presence or absence of MMI-0100 peptide; 0 µM (vehicle only, 0.1% DMSO final), 20 µMand 100 µM MMI-0100 peptide. **C.** LDH detection in media from the same experimental conditions as the caspase activity described above. A Kruskal-Wallis One-way ANOVA was performed at each terminal time point in experiments setup and ran in parallel. If significance was reached ($p<0.05$), a post-hoc all pairwise Multiple Comparison Procedures (Tukey Test) was performed between each of the groups to determine significance. *$p<0.05$ vs. 0 µM group (DMSO vehicle control); **$p<0.05$ vs. other two groups; *** $p<0.05$ vs. 20 µM MMI-0100 peptide group.

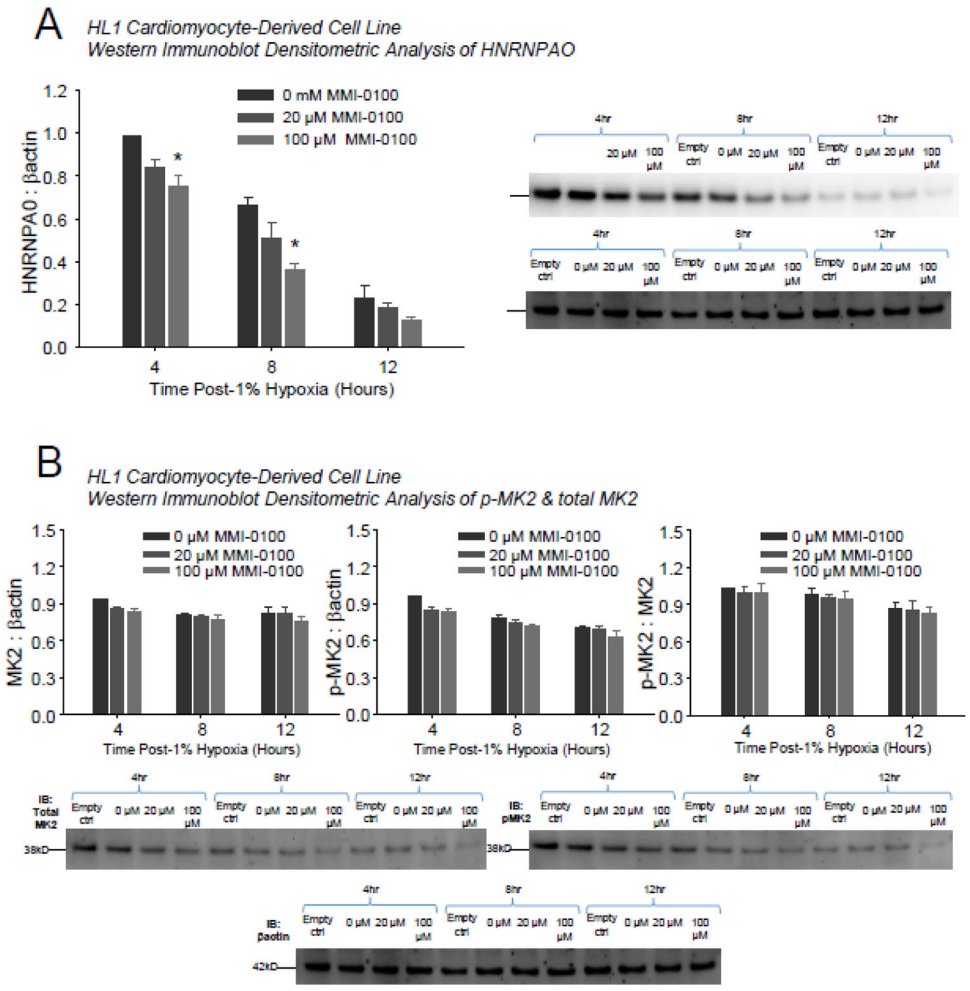

Figure 6.

In HL1 cardiomyocytes challenged with 1% hypoxia, MMI-0100 peptide reduces MK2 activity measured by downstream HNRNPA0 protein expressed, but not phospho- or total MK2 levels. A. H9C2 cells were challenged with 1% hypoxia for 4, 8, and 12 hours; desitometric analysis of Western immunoblot (right, representative 1 of 3 replicates per bar) demonstrated significant decreases in HNRNPA0 protein expression. B. Densitometric analysis phospho- and total MK2 levels (below). A Kruskal-Wallis One-way ANOVA was performed at each terminal time point in experiments setup and ran in parallel. If significance was reached ($p<0.05$), a post-hoc all pairwise Multiple Comparison Procedures (Tukey Test) was performed between each of the groups to determine significance. *$p<0.05$ vs. 0 μM group (DMSO vehicle control).

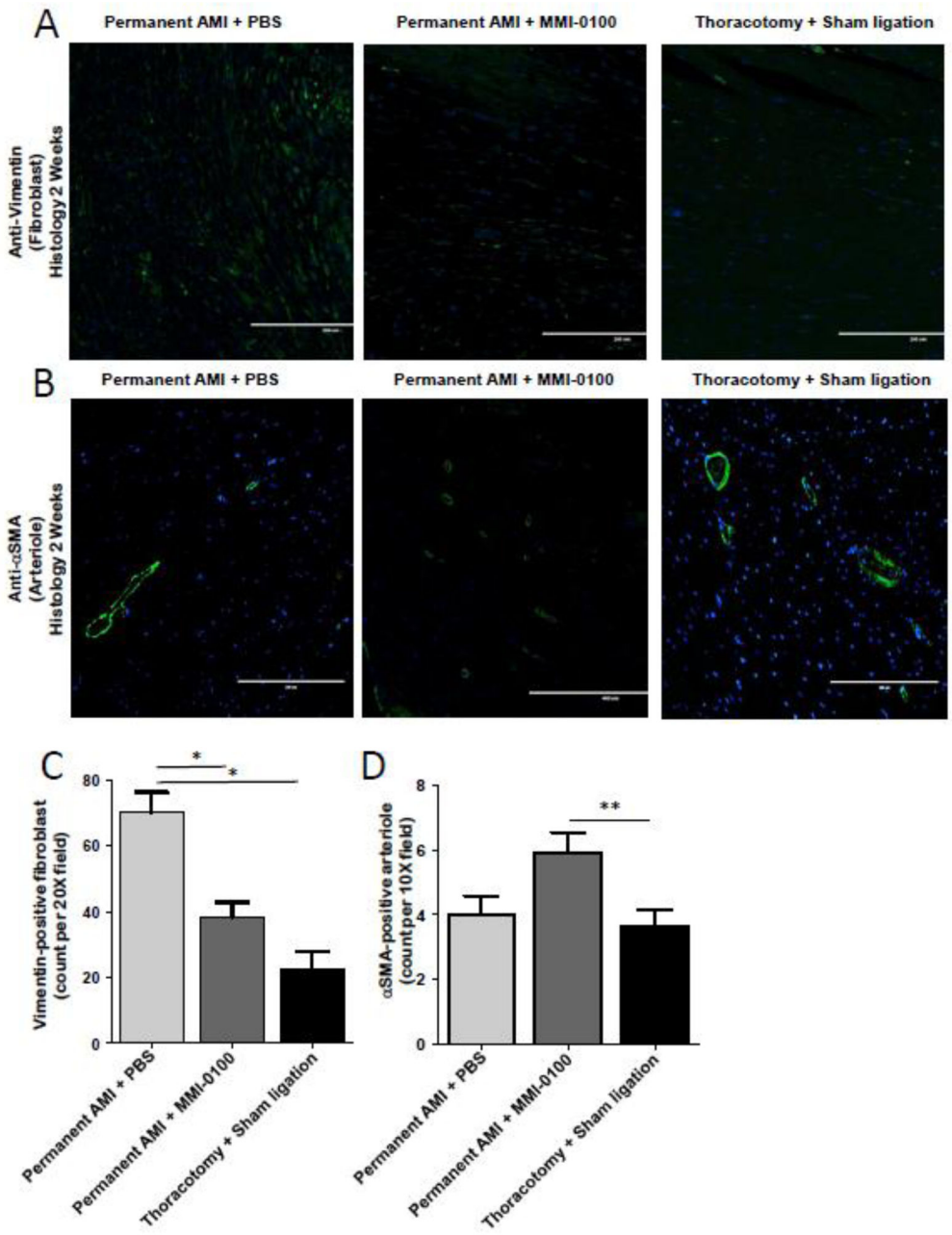

Figure 7.

MMI-0100 reduces the number of vimentin-positive fibroblast cells and increases vessel density two weeks after chronic AMI. Quantification of cardiac fibroblasts and vessels was detected by immunofluorescence using anti-vimentin and anti-α-smooth muscle actin (αSMA), respectively from serial sections in hearts reported in Figure 1 and Figure 2. MI only (permanent AMI + Daily PBS), MMI-0100 (permanent AMI + daily MMI-0100), and Sham (Thoractomy +Sham Ligation) sections from 3 independent animals per group were quantitatively analyzed. Microphotographs of representative **A.** anti-vimentin and **B.** anti-α-smooth muscle actin immunofluorescence illustrate that MMI-0100 treatment after MI **C.** reduces vimentin positive fibroblasts and **D.** increases αSMA-positive arterioles. Staining

positive cells was calculated by using Meta-Morph analysis software (Molecular Devices, Sunnyvale, CA) quantitative unbiased software with the average value of at least 4 random fields from each section in double-blind fashion. The relative number of positive cells identified determined the relative numbers of αSMA, vimentin, and TGF-β1-positive cells. Groups were statistically compared using a One-Way ANOVA, followed by a post-hoc multiple comparisons test (Tukey's Test). *$p<0.001$ vs. all other groups.

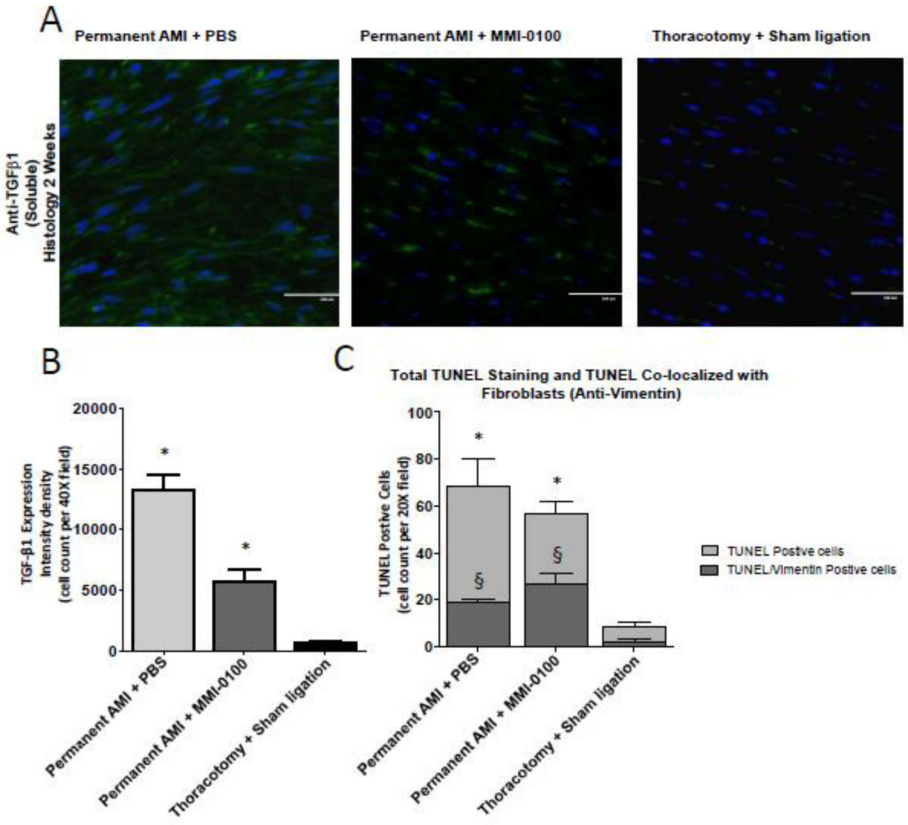

Figure 8.

MMI-0100 reduces the number of TGF-β1-positive fibroblast cells and decreases the total number of TUNEL positive cells, despite a relative increase in TUNEL positive fibroblasts two weeks after chronic AMI. Quantification of TGF-β1-positive cells was detected by immunofluorescence and apoptosis was detected by TUNEL staining and co-localization with anti-vimentin (fibroblasts) from serial sections in hearts reported in Figure 1 and Figure 2. MI only (permanent AMI + Daily PBS), MMI-0100 (permanent AMI + daily MMI-0100), and Sham (Thoractomy +Sham Ligation) sections from 3 independent animals per group were quantitatively analyzed. Microphotographs of representative **A.** anti-TGF-β1 and quantification of **B.** TGF-β1-positive cells, and **C.** the total TUNEL positive cells (light gray) that co-stain with anti-vimentin (fibroblasts) illustrating the effects of MMI-0100 treatment after chronic AMI C. reduces vimentin positive fibroblasts and D. increases αSMA-positive arterioles. The number of positively stained cells was calculated by using sing Meta-Morph analysis software (Molecular Devices, Sunnyvale, CA) quantitative unbiased software with the average value of at least 4 random fields from each section in double-blind fashion. The relative number of positive cells identified determined the relative numbers of TGF-β1–, TUNEL-, and vimentin-positive cells histologically. Staining was quantified using MetaMorph software analysis by identification of tissue apoptotic nuclei in 10 random fields for each individual mouse. A One-Way ANOVA was used to analyze differences in TGF-β1; a Two-Way ANOVA was used to analyze the role of MMI-0100 on

TUNEL–positivity and the role of fibroblasts in these changes. *p<0.001 vs. all other groups (all TUNEL positive cells in C); §p<0.001 vs. other vimentin-positive cells in other groups.

J Mol Cell Cardiol. Author manuscript; available in PMC 2015 December 01.

Table 1

Echocardiographic analysis of conscious C57BL/6 mice at baseline (pre-treatment), 1 week, and 2 weeks after thoracotomy and sham ligation (Group 1) or acute MI (complete, permanent ligation of left anterior descending (LAD) coronary artery) with daily intraperitoneal MMI-0100 or vehicle control (PBS)

A Kruskal-Wallis One-way ANOVA was performed at each time point in experiments setup and ran in parallel. If significance was reached ($p<0.05$), a post-hoc all pairwise Multiple Comparison Procedures (Tukey Test) was performed between each of the groups to determine significance. *$p<0.01$ vs. Group 1. **$p<0.05$ vs. vs acute myocardial infarction (AMI=permanent ligation of LAD) + PBS.

M mode Measure	C57BL/6 Baseline Group 1 AMI + PBS N=6	C57BL/6 Baseline Group 2 Thoracotomy + Sham Ligation Vehicle N=6	C57BL/6 Baseline Group 3 AMI + MMI-0100 N=3	C57BL/6 1 Week Group 1 AMI + PBS N=8	C57BL/6 1 Week Group 2 Thoracotomy + Sham Ligation Vehicle N=6	C57BL/6 1 Week Group 3 AMI + MMI-0100 N=8	C57BL/6 2 Weeks Group 1 AMI + PBS N=8	C57BL/6 2 Weeks Group 2 Thoracotomy + Sham Ligation Vehicle N=6	C57BL/6 2 Weeks Group 3 AMI + MMI-0100 N=7
AWTD (mm)	1.14±0.03	1.10±0.02	1.13±0.03	1.06±0.07	1.07±0.04	1.21±0.03	1.07±0.08	1.12±0.01	1.00±0.10
AWSTS (mm)	1.76±0.02	1.73±0.05	1.77±0.03	1.59±0.16	1.64±0.05	1.84±0.08	1.54±0.14	1.72±0.02	1.49±0.21
LVEDD (mm)	2.79±0.18	2.61±0.13	2.66±0.07	4.04±0.23	3.03±0.09*	3.43±0.13*	3.99±0.24	2.81+0.07*	3.74±0.09*
LVESD (mm)	1.24±0.10	1.12±0.06	1.18±0.06	2.73±0.22	1.43±0.04*	1.91±0.14*	2.88±0.29	1.22±0.05*	2.43±0.14*
PWTD (mm)	1.06±0.03	1.04±0.03	0.98±0.04	0.87±0.04	0.98±0.01	1.15±0.04	0.96±0.08	1.02±0.02	1.17±0.04*
PWTS (mm)	1.86±0.05	1.86±0.06	1.78±0.15	1.44±0.07	1.71±0.05*	1.72±0.09*	1.43±0.11	1.73±0.04*	1.75±0.04*
EF (%)	87.4±1.3	88.5±1.0	87.6±0.9	61.8±2.5	85.2±0.6*	76.4±2.82*,**	54.6±4.4	88.0±1.4*	64.9±3.4**
FS (%)	55.7±1.7	57.0±1.4	55.7±1.2	33.0±1.8	52.9±0.7*	44.7±2.6*,**	28.3±2.8	56.6±1.9*	35.3±2.4**
LV Vol;d (μl)	30.3±4.2	25.3±3.3	26.1±1.6	74.5±10.4	36.2±2.6*	49.3±4.4*	71.1±10.9	30.0±2.0*	60.1±3.5**
LV Vol;s (μl)	3.9±4.2	2.9±0.4	3.3±0.4	3.9±5.9	5.4±0.4	12.1±2.2	35.2±9.2	3.6±0.4*	21.7±3.2
LV Mass (mg)	108.8±8.4	95.3±10.0	95.1±4.7	160.2±19.9	109.4±5.5*	162.2±8.4	169.4±5.5	104.4±4.4 (p=0.094)	162.7±13.2
LV Mass/Bo dy Weight (mg/g)	3.9±0.3	3.7±0.30	4.0±0.2	6.2±0.9	4.2±0.2	6.5±0.2	6.7±1.6	3.8±0.1	6.3±0.5
HR (bpm)	684±12	681±21	699±7	647±23	690±10	638±14	680±25	712±4	689±13

bpm, beats per minute; LV mass index [(ExLVD^{3}d-LVED^{3}d) × 1.055]; HR, heart rate; AWTD, anterior wall thickness in diastole; AWSTS, anterior wall thickness in systole; PWTD, posterior wall thickness in diastole; PWTS, posterior wall thickness in systole; LVEDD, left ventricular end-diastolic dimension; LVESD, left ventricular end-systolic dimension; LV Vol;d, LV volume in diastole; LV Vol;s,, LV volume in systole; FS, fractional shortening, calculated as (LVEDD-LVESD)/LVEDD × 100; EF%, ejection fraction calculated as (end Simpson's diastolic volume – end Simpson's systolic volume)/end Simpson's diastolic volume * 100.

Table 2

Echocardiographic analysis of conscious C57BL/6 mice at baseline (pre-treatment), 1 week, and 2 weeks of daily intraperitoneal MMI-0100 or vehicle control (PBS)

A Student's t-test was performed to compare the two groups at each time point ($p<0.05$).

M mode Measure	C57BL/6 Baseline Daily PBS Vehicle N=3	C57BL/6 Baseline Daily MMI-0100 N=9	C57BL/6 1 Week Daily PBS Vehicle N=3	C57BL/6 1 Week Daily MMI-0100 N=12	C57BL/6 2 Weeks Daily PBS Vehicle N=3	C57BL/6 2 Weeks Baseline Daily MMI-0100 N=12
AWTD (mm)	1.03±0.05	1.17±0.03	1.08±0.02	1.10±0.03	1.13±0.02	1.13±0.06
AWSTS (mm)	1.74±0.15	1.79±0.03	1.72±0.02	1.74±0.03	1.76±0.02	1.66±0.07
PWTD (mm)	1.06±0.03	1.05±0.05	1.00±0.02	1.08±0.03	1.03±0.02	1.04±0.08
PWTS (mm)	1.67±0.03	1.72±0.09	1.75±0.03	1.87±0.03	1.77±0.03	1.79±0.05
LV Mass (mg)	118.8±6.5	106.4±7.9	81.6±3.9	91.2±4.6	85.0±2.5	74.0±9.1
LV Mass/Body Weight (mg/g)	4.4±0.2	3.9±0.3	3.8±0.2	3.1±1.0	3.9±0.1	3.2±0.4
HR (bpm)	670±23	658±19	672±9	684±10	706±9	729±6

Bpm, beats per minute; LV mass index [(ExLVD^{3}d-LVED^{3}d) × 1.055]; HR, heart rate; AWTD, anterior wall thickness in diastole; AWSTS, anterior wall thickness in systole; PWTD, posterior wall thickness in diastole; PWTS, posterior wall thickness in systole; LVEDD, left ventricular end-diastolic dimension; LVESD, left ventricular end-systolic dimension; LV Vol;d, LV volume in diastole; LV Vol;s,, LV volume in systole; FS, fractional shortening, calculated as (LVEDD-LVESD)/LVEDD × 100; EF%, ejection fraction calculated as (end Simpson's diastolic volume – end Simpson's systolic volume)/end Simpson's diastolic volume * 100.